Int. J. Heat Mass Transfer. Vol. 30, No. 1, pp. 109–124, 1987
Printed in Great Britain

0017–9310/87 $3.00 + 0.00
Pergamon Journals Ltd.

Thermocapillary periodic flows

A. G. KIRDYASHKIN
Institute of Geology and Geophysics, Siberian Branch of the U.S.S.R. Academy of Sciences, 630090, Novosibirsk, U.S.S.R.

(*Received* 14 *October* 1985)

Abstract—This paper describes experimental investigations of the structure of periodic thermocapillary flows originating from periodic variations of heat flux on a linear source located at a free surface. The periodic flows develop in a plane horizontal layer with adiabatic horizontal surfaces for which the trends in convective flow far from the heat sources are known. The temperature fields are measured at different periods and amplitudes of the change in heat flux. The instantaneous and mean temperature gradients are measured along a free surface and, hence, the friction on the surface. The limits of the propagation of periodic perturbations depending on the amplitude and period of change in loading are found. It is shown that for $t_0 < 35$ s the thermogravitational forces do not exert a noticeable effect on the propagation of a periodic flow along the free surface.

INTRODUCTION

THERMOCAPILLARY forces originate on non-isothermal, free surfaces of pure liquids that do not absorb surfactants capable of suppressing the thermocapillary effect. The surface thermocapillary forces brought about by temperature-induced changes in the surface tension have the nature of molecular interaction and are of low-inertia character. Thermal gravitational flows caused by body forces due to temperature-induced changes in the liquid density in a gravitational field have higher inertia than the thermocapillary flows.

An interaction between thermocapillary and thermogravitational forces takes place. For example, under the conditions of steady-state flow in a horizontal layer the relationship between thermocapillary and thermogravitational forces induced in a horizontal layer by a horizontal temperature gradient in the mode of plane-parallel flow (heat conduction regime) is characterized by the dimensionless group [1, 2]

$$k = Ma/Ra = b/\rho\beta g l^2.$$

In other flow conditions the interaction between these forces is not susceptible to such a simple one-parameter estimation.

A more complex interplay of these forces can be expected in unsteady-state flow conditions (for example, periodic regimes) as being most regular and therefore more accessible for the study of the interaction between thermocapillary and thermogravitational forces in unsteady-state conditions.

Because of a substantial difference between the times of relaxation of thermocapillary and thermogravitational flows at different periods of change in the heat exchanger temperature near a free surface, the contribution of thermocapillary and thermogravitational forces will be different and, because of their low inertia, the influence of thermocapillary forces will increase with an increasing frequency of oscillation.

Thermocapillary and thermogravitational flows in a horizontal layer do not have the stability threshold and originate at arbitrarily small horizontal temperature gradients.

The absence of the stability threshold simplifies the problem of studying the interaction between these forces in unsteady-state conditions, therefore it is worthwhile studying the structure of these flows in horizontal layers with adiabatic horizontal surfaces, especially since the steady-state flow conditions have received the most study for this case [2].

The structure of thermocapillary periodic flows is of interest in view of optimizing the conditions for obtaining monocrystals. Use is made of the methods of growing monocrystals from melts or solutions when there are free surfaces on which steady-state and periodic thermocapillary flows may develop [3]. These originate on periodic change in the heat flux on a heater near a free surface. When the boundary-layer flow near the vertical heating surfaces loses its stability, unsteady-state variations of temperature at the free surface near the wall are observed which generate unsteady-state thermocapillary flows. Thermocapillary periodic flows develop near the free surface of melt in the process of monocrystal growing by the Chokhralsky method. Because of the non-alignment of the crystal axes and the crucible during the rotation of the former or of the latter, the temperature varies periodically at each point around the perimeter of crystal wetting by the melt and this causes periodic flows. The interaction of thermal, gravitational and thermocapillary forces is observed in all cases.

Experimental investigations of the structure of periodic thermogravitational flows in a horizontal layer with two rigid boundaries are reported in refs. [4, 5]. The periodic flows were created by modulating the

NOMENCLATURE

A	horizontal temperature gradient
a	thermal diffusivity
b	temperature coefficient of surface tension, $\partial\sigma/\partial T$
c_p	heat capacity at constant pressure
g	free fall acceleration
$2l$	height of a layer
Ma	Marangoni number, $bl\Delta T/\rho va$
$\bar{Q}$	mean heat flux for a period
Ra	Rayleigh number, $\beta g\Delta Tl^3/av$
T	temperature
ΔT	difference of temperatures between the upper and lower horizontal adiabatic surfaces
T_l, T_{-l}	temperatures of the upper and lower horizontal adiabatic surfaces
T_c	temperature of the vertical cold surface
t	time
t_o	period of the oscillations of heat flux
t_φ	temporal shift of the maximum temperature phase, T_m
u	horizontal velocity component
u_φ	phase velocity of maximum temperature
y, x, z	vertical and horizontal coordinates
x_1, z_1	length and width of a seal
x_o	distance of periodic flow propagation.

Greek symbols

β	coefficient of thermal expansion of liquid
θ	dimensionless temperature at $x = \text{const}$, $= (T-T_{-l})/\Delta T$
μ, ν	dynamic and kinematic viscosities
ρ	density
σ	coefficient of surface tension
τ_o	friction factor on a free surface.

Subscripts and other symbols

o	free surface of liquid
m	maximum
-	average value.

temperature of a side wall at sub- and supercritical Rayleigh numbers in the horizontal layer.

The methods of numerical simulation were used to investigate the structure of periodic thermogravitational flows in the horizontal layer under different boundary conditions on horizontal surfaces [6, 7].

The results on flow stability in the horizontal layer in the conditions of thermocapillary and thermogravitational convection are presented in refs. [8, 9] under the boundary conditions first formulated in ref. [1]. In the absence of temperature difference between the horizontal surfaces, solutions are obtained for the temperature and velocity distributions over the layer thickness and the heat transfer conditions on horizontal surfaces are found in which a constant horizontal temperature gradient exists over the entire layer. The development of finite-amplitude perturbations in the horizontal layer for the above-mentioned flow is treated in ref. [10]. The stability of a plane-parallel flow under different conditions on a free surface is studied in ref. [11]. The steady- and unsteady-state thermocapillary flows on a cylindrical free surface when its generatrices are parallel to the gravity force vector are studied experimentally in ref. [12]. In ref. [13] an asymptotic theory is presented for an elongated layer and a numerical experiment for a rectangular cavity when there are free surfaces and the motion originates under the action of thermocapillary forces.

A survey of the works on theoretical and experimental investigations and numerical experiments in a horizontal layer with rigid adiabatic bounding surfaces in the case of side heating with free convection is given in ref. [14].

The present paper describes experimental investigations into the structure of periodic thermocapillary flows originating due to periodic variations of the heat flux on a linear source located near the free surface of the liquid. Periodic flows develop in a plane horizontal layer (with adiabatic horizontal surfaces), for which the laws governing the convective flow far from a heat source have been already studied. Instantaneous and mean temperature gradients have been measured along the free surface and, hence, the friction on the surface. The limits of the propagation of periodic perturbations depending on the amplitude and period of power variation have been found. It is shown that for $t_o < 35$ s the thermogravitational forces do not exert a noticeable effect on the periodic flow propagation along the surface.

STATEMENT OF THE PROBLEM AND EXPERIMENTAL FACILITY

Thermocapillary periodic flows were set up in a plane horizontal layer with thermally insulated surfaces. The schematic diagram and boundary conditions are presented in Fig. 1. The working fluid is a 96% ethyl alcohol solution on whose non-isothermal free surface thermocapillary forces originate [2]. The experimental set-up is a tank made of optically transparent acrylic plastic with horizontal dimensions $x_1 = 380$ mm, $z_1 = 150$ mm (the construction is described elsewhere [2]).

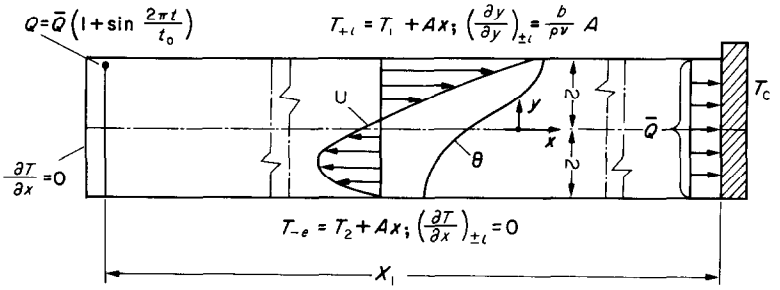

FIG. 1. Boundary conditions in a horizontal layer in the study of periodic flows.

The upper, thermally insulated, horizontal plate was fabricated from two acrylic plastic plates ($3\times148\times380$ mm^3) in such a way that a $15\times125\times360$ mm^3 cavity filled with foam plastic was left between them. The horizontal plate had optically transparent slits ($\delta=3$ mm) along its entire length at distances $z=45$ and 75 mm from the forward optically transparent end face. The thickness of the liquid layer ($2l$) and of the upper air layer (δ_a) was set with the aid of four calibrated plates, placed into the tank, that were 3 mm thick, 10 mm long and $2l+\delta_a$ high, and on which the upper horizontal plate was mounted. Once the upper horizontal plate had been positioned on the calibrated plates, the gaps between the tank and the plate were taped, to isolate the working layer from the ambient air, so that almost no evaporation of the working liquid was noted in the course of the entire experiment lasting for 9–10 h.

The working volume of the tank was filled with liquid up to the required height, but so that the liquid was not in contact with the upper plate. The distance from the free surface of the liquid to the upper insulating horizontal plate was $\delta_a\approx10$ mm. The horizontal position of the tank was regulated by set screws and was controlled by a B-630 cathetometer accurate to 0.01 mm. On its one vertical end a copper heat exchanger was installed whose constant temperature was ensured by a temperature-controlled water circulating in its cavity. A U-10 thermostat was used which maintained the constant temperature within ±0.03°C.

A 0.15-mm-diameter, 145-mm-long nichrome wire, stretched between two elastic holders, was used as a heater. The wire was positioned horizontally at a distance of 5 mm along the vertical, thermally insulated end and at a distance of 0.2 mm from the free surface.

The system for controlling the supplied periodic voltage on loading is presented in Fig. 2(a). The frequency of voltage oscillations was set by a low-frequency generator (3), the range of its oscillation period regulation being 0.2–100 s. The amplitude of periodic power was set by a power amplifier (2) and was regulated within the range 0–45 W. Constant voltage was fed from an IPN-21 (5). The signal frequency was controlled with the aid of an F 5041 digital frequency meter–chronometer (6). The power supplied to the heater (a 0.15-mm-diameter nichrome wire) can be formulated by the law

$$Q=Q_1+\bar{Q}\left(1+\sin\frac{2\pi t}{t_0}\right) \tag{1}$$

where $0.2<t_0<100$ s.

In the steady-state flow region the temperature in the layer was measured by a thermocouple probe made from 0.05-mm-diameter nichrome–constantan wires. The vertical part of the Γ-like probe was a metallic pipe, 3 mm in diameter and 250 mm long, into which the thermocouple wires were inserted. The horizontal part of the probe was made of a two-channel capillary, 1.5 mm in diameter and 70 mm long. The free ends of the thermocouple wires were 15 mm long. The Γ-like probe moved in the vertical direction together with a coordinate plate measuring $13.5\times14\times200$ mm^3 and was inserted into a 14×14 mm^2 milled recess in the rear wall of the tank. The

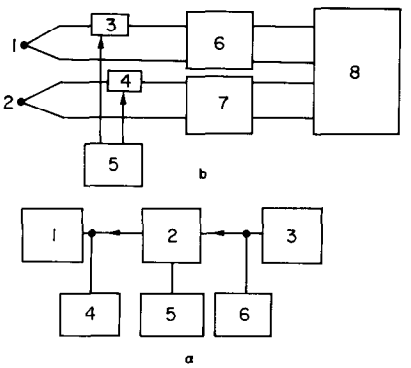

FIG. 2. (a) Flow chart of regulation and control of periodic power: 1, heater; 2, power amplifier; 3, low-frequency generator; 4, oscilloscope; 5, constant current source; 6, frequency meter–chronometer. (b) Flow chart of the measurement of instantaneous temperatures in the layer: 1, 2, thermocouples; 3, 4, compensating potentiometers; 5, voltage comparator; 6, 7, constant current amplifiers; 8, two-channel self-recording potentiometer.

recesses were spaced at 50-mm intervals along the layer. The thermocouple could be moved in the horizontal plane by rotating the probe around its vertical axis. The displacement of the thermocouple probe along the vertical was controlled by a V-630 cathetometer accurate to within 0.01 mm. The e.m.f. of the thermocouple was measured by a P 3003 comparator with an accuracy of 0.5 μV. To measure instantaneous temperatures and correlations along x and y in the layer, two 0.05-mm-diameter nichrome–constantan thermocouples were used. The Γ-like thermocouple probes were inserted through a 3-mm-wide and 200-mm-long slit milled in the upper thermally insulated plate at a distance of $z = 90$ mm from the frontal end face. Over x, the thermocouple probes moved along 8×20 mm^2 tracks. Each thermocouple could move independently of one another along (x) and across (y) the layer and could rotate around their own axes over x and z. The free end of the needle-type thermocouple was 20 mm long. The thermocouple traversal across the layer was controlled with the aid of a cathetometer accurate to within 0.01 mm. The displacement of thermocouples along x relative to one another was checked with an accuracy of 0.2 mm by the cathetometer using the calibrated graduations on the optical scale. The cold junction of the thermocouple had the temperature of the temperature-controlled cooling water circulating in the heat exchanger cavity. These probes were used to measure instantaneous temperature differences in the layer relative to the cooling surface of the copper heat exchanger whose walls were 0.5 mm thick.

The flow charts depicting simultaneous measurements of the instantaneous e.m.f.s. of the thermocouples are given in Fig. 2(b). The e.m.f. constant component of thermocouples (1) and (2) was compensated and measured by small-size potentiometers (3) and (4) which had been calibrated with the aid of an R 3003 comparator (5) accurate to 0.5 μV. The non-compensated e.m.f. component (with the comparator switched off) was strengthened by constant-current amplifiers (7) and (6) with a smoothly regulated gain K. To reduce the level of noise, the signal, after the constant-current amplifier, was passed through a low-frequency filter with a cut-off frequency of 1.5 Hz. The constant-current amplifiers had low noise (reduced to the second amplifier, i.e. 1 μV) and the drift of 1 μV h^{-1}. Analog signals of thermocouples were recorded simultaneously on a H 3P21-2 two-channel recorder.

The instantaneous local temperatures in the layer relative to the cooling heat exchanger surface T_c were determined from the formula

$$T = T_t - T_c = \left(\Delta U_k + \frac{\Delta U_t}{K}\right) \Big/ R \qquad (2)$$

where U_k is the compensated constant component of the e.m.f. measured by potentiometers (3) and (4); ΔU_t is the non-compensated, amplified portion of the e.m.f. of the thermocouple; K is the gain of the system measured by calibration against the resistance equivalent to that of the thermocouple; R is the thermocouple constant (sensitivity, μV °C^{-1}).

The instantaneous temperature gradient $(\partial T/\partial x)_0$ on the free surface of the layer was measured with the aid of a differential thermocouple made of 0.05-mm-diameter nichrome–constantan wires. Constructionally the Γ-like thermocouple probe was made the same way as the thermocouple measuring instantaneous temperatures and moved in the same coordinate system. The junctions of the needle-type differential thermocouple were arranged in one horizontal plane at a distance of 6 mm from one another. The rotation of the probe around its axis made it possible to vary the distance between the thermocouple junctions along $x(\Delta x)$ being controlled by a cathetometer. The instantaneous value of the e.m.f. of the differential thermocouple was measured at the known distance between the thermocouple junctions (Δx).

The temperature gradient on the free surface was determined by the formula

$$\left(\frac{\partial T}{\partial x}\right)_0 = \frac{\Delta U_t}{K \cdot R \cdot \Delta x}. \qquad (3)$$

Instantaneous e.m.f.s of the differential thermocouple undergo reversal of sign and can be both positive and negative for the period. It becomes important in this case that the measuring system could be accurately set to zero. This was done by including into the system the resistance equivalent to that of the thermocouple and by disconnecting the thermocouple. With thorough screening of the differential thermocouple, its spurious constant component in isothermal conditions amounted to about 2 μV. To eliminate this type of inaccuracy, the e.m.f. analog amplified signal of the differential thermocouple was recorded during the change of its polarity. Analog periodic signals on the change of polarity are mirror images of one another. The symmetry line of these two analog recordings of the e.m.f. of the differential thermocouple is the line of zero value.

The liquid flow velocity in the layer was measured with the aid of flow visualization by using aluminum particles that were in the flow during the entire experiment lasting for 9–10 h. The layer with the particles was transparent through its entire width, z_1. The steady flow velocity was determined by the time for which the particle passed a fixed distance on the graticule of the cathetometer viewing tube.

RESULTS OF MEASUREMENTS AND THEIR ANALYSIS

1. *Steady-state flow far from a heater*

Experimental investigations were carried out in a layer of ethyl alcohol with $2l = 10$ mm, $x_1 = 380$ mm, $z_1 = 150$ mm and insulated horizontal surfaces (Fig. 1).

A horizontal temperature gradient induces ther-

mocapillary forces on the upper free surface [2]:

$$\frac{\tau_0}{\rho}=\frac{b}{\rho}\left(\frac{\partial T}{\partial x}\right)_0;\quad \left(\frac{\partial u}{\partial y}\right)_0=\frac{b}{\mu}\left(\frac{\partial T}{\partial x}\right)_0 \tag{4}$$

where b is a negative quantity. For ethyl alcohol $b=-9\times10^{-5}$ N m^{-1} deg^{-1}.

It is shown [2] that in the case of a developed flow far from the end faces in a layer with thermally insulated, horizontal surfaces, the initial parameters of the problem are the heat flux (or the temperature drop on adiabatic surfaces) and the height of the layer. Then the knowledge of the flow structure near the end faces of heat exchanging surfaces is not required. In such a layer the flow originates under the action of thermocapillary and thermogravitational forces the relationship between which is governed by the parameter $k=Ma/Ra$. Under the boundary conditions, presented in Fig. 1, and at $Q=$ const. the following solutions are obtained for the plane-parallel flow region [2]:

$$A=(\partial T/\partial x)=\pm[30/(3-5k)Ra]^{1/2} \tag{5}$$

$$u=-[30/(3-5k)Ra]^{1/2}\times\left[\frac{y^3}{6}+\frac{3k-1}{8}y^2+\frac{k-1}{4}y-\frac{3k-1}{24}\right] \tag{6}$$

$$\theta=\frac{5}{12-20k}\left[\frac{y^5}{5}-\frac{3k-1}{4}y^4+(k-1)y^3+\frac{1-3k}{2}y^2+(2-3k)y-\frac{5k}{4}+\frac{19}{20}\right] \tag{7}$$

$$(T-T_2)/\Delta T=\theta+Ax \tag{8}$$

where l is the length scale; $\Delta T=T_l-T_{-l}=T_1-T_2$ is the temperature scale; $Ra(a/l)$ is the velocity scale; T_2 is the temperature on the lower surface for the known value of x. The velocity and temperature fields were investigated at the steady power $\bar{Q}=45.5$ W m^{-1} supplied to the nichrome wire at the free surface. Figure 3 presents the results of measurements of the velocity (a) and temperature (b) profiles in the layer for different cross-sections x ($T_2=25.7$°C at $x=125$ mm). A good coincidence between the measured and predicted velocity and temperature profiles far from the end face, $x>2l$, is observed. The value of $(\partial T/\partial x)_0$ obtained experimentally and calculated from equation (5) is equal to -7.8°C m^{-1}. Near the heater ($x<15$ mm) the temperature fluctuations observed are caused by unstable stratification due to a high temperature at the heater and heat removal into a gas interlayer. The investigations were subsequently carried out for $\bar{Q}<27$ W m^{-1} in order to eliminate

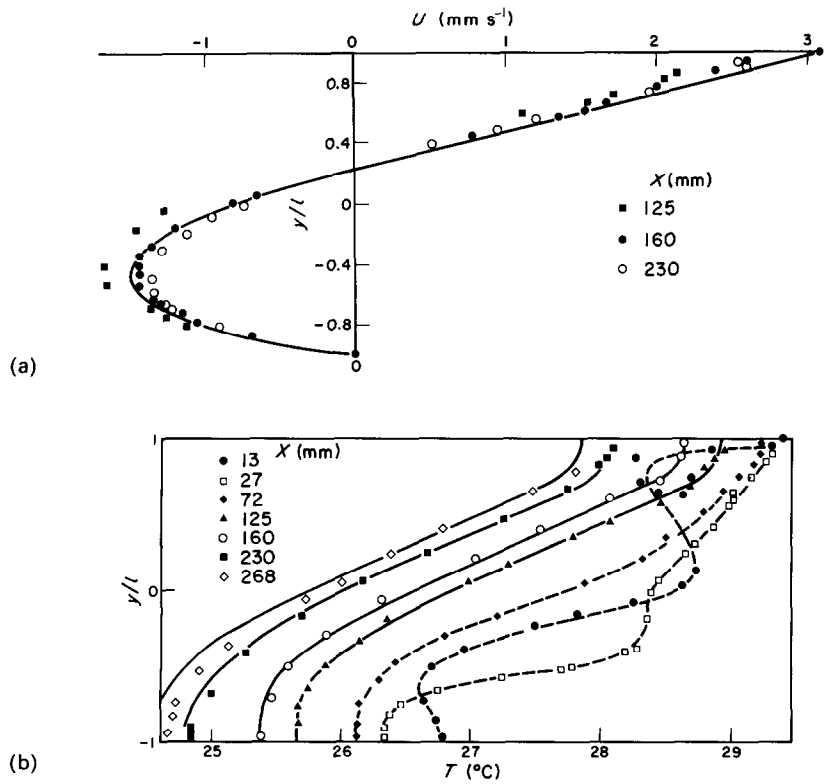

FIG. 3. Velocity (a) and temperature (b) profiles in a horizontal layer with a free upper boundary at a constant heat flux $\bar{Q}=45.5$ W m^{-1}, $2l=10.1$ mm, $-Ma=1.63\times10^4$, $Ra=3.9\times10^4$, $k=-0.42$, $T_c=20.6$°C. Solid lines, calculation by equation (6) for (a) and by equations (5), (7) and (8) for (b).

the effect of heat transfer into the gas interlayer close to the heater.

Figure 21(a) shows the flow pattern in the vicinity of the heater at a steady-state power. A strong steady eddy flow is due to thermocapillary forces. These are substantial because of a high temperature gradient $(\partial T/\partial x)_0$ near the heater. The longitudinal vortex dimension is $x_a/l = 5$.

2. *Periodic flows at* $t_0 = 3$ s

The structure of periodic flows was investigated in the absence of the constant component of power $Q_1 = 0$, equation (1):

$$Q = \bar{Q}\left(1 + \sin\frac{2\pi t}{t_0}\right) \tag{9}$$

and $2 \leqslant t_0 \leqslant 35$ s. The working volume was filled with liquid and the heater (nichrome wire) was immersed into it to a depth of 0.2 mm from the free surface. On positioning the wire close to the surface so that the destruction of the free surface plane is observed, the liquid near the heater at Q_m becomes superheated and starts to evaporate. Measurements were started 3.5 h after the supply of periodic voltage to the loading.

The results of experimental studies for $t_0 = 3$ s, $2l = 10.1$ mm, $\bar{Q} = 21.04$ W m^{-1}, $Ma = -9.2 \times 10^3$, $Ra = 2.1 \times 10^4$, $k = -0.434$, $T = 2°C$, $T_c = 20.1°C$ are presented in Figs. 4–11 and 21(b). The free surface temperature was measured by two thermocouples one of which was fixed and the other moved along x in the same plane: $z = \text{const}$. Figure 4 gives instantaneous temperatures on the free surface at different distances from the periodic heat flux source, as well as the phase shift at different values of x. The temperature varies strictly periodically in time at all the values of x, decreasing in amplitude with distance from the heater. The amplitude and mean values of the temperature as functions of x are presented in Fig. 5. The instantaneous temperatures at any values of t/t_0 and x can be determined from the plots of Figs. 4 and 5. Figure 6 presents the measured phase shift of the maximum temperature t_φ/t_0 at different values of x and the phase velocity of the maximum temperature $u_\varphi = \partial x/\partial t_\varphi$.

When the phase of the maximum temperature shifts by one period ($x = 27$ mm), the amplitude value of temperature decreases to $0.1\Delta T$ (Fig. 5), the phase velocity decreases down to the doubled value of the velocity on the free surface [Figs. 6 and 11(I)]. At $x = 38.5$ mm the amplitude value of temperature fluctuation becomes commensurable with the resolving power of temperature measurements, however, the phase shift (for T_m) can be well traced and constitutes $t_\varphi/t_0 = 2$; the phase velocity is commensurable with the liquid surface flow velocity in the developed flow region far from the heater [Fig. 11(I)].

The mean temperature gradient (at $y = 1$, Fig. 5) in the periodic flow region varies non-monotonously: when $4 < x < 10$ mm, $\bar{A}_0 > 0$; in the region of fluctuation attenuation $\bar{A}_0 = 0$. In the developed flow the

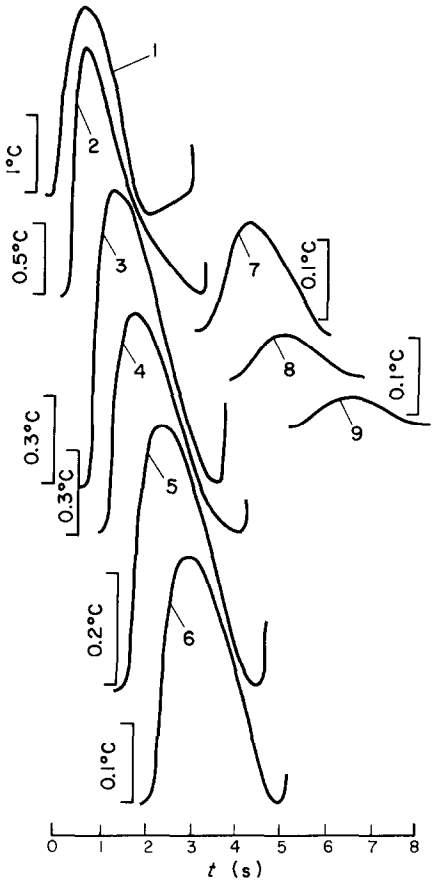

FIG. 4. Variation of the free surface temperature ($y = 1$) in time for different distances (x) from the heater in the layer of $2l = 10.1$ mm. $\bar{Q} = 21.04$ W mm^{-1}, $-Ma = 9.2 \times 10^3$, $Ra = 2.1 \times 10^4$, $k = -0.434$, $T_c = 20.1°C$, $t_0 = 3$ s. (1) $x = 2.25$ mm; (2) 6.25 mm; (3) 12.5 mm; (4) 16 mm; (5) 20.5 mm; (6) 24 mm; (7) 28.5 mm; (8) 32 mm; (9) 36.5 mm.

experimental values of $A = -0.007°C$ mm^{-1} [by formula (5), $A = -0.0066°C$ mm^{-1}]. According to Fig. 5 and relations (4), when $4 < x < 10$ mm, the averaged friction coefficients due to thermocapillary forces have negative values, $\bar{\tau}_0 < 0$ and $(\partial\bar{u}/\partial y)_0 < 0$. In this region over x the averaged motion on the surface can be directed to the heater and $\bar{u}_0 < 0$.

Instantaneous temperature gradients on the free surface, $(\partial T/\partial x)_0$, were measured and mean values, $(\partial\bar{T}/\partial x)_0$, were found. The friction factors due to thermocapillary forces and velocity gradients normal to the surface, τ_0/ρ, $\bar{\tau}_0/\rho$, $(\partial u/\partial y)_0$, $(\partial\bar{u}/\partial y)_0$, were determined from relations (4).

The longitudinal temperature gradient $\partial T/\partial x$ at different distances from the free surface, $\Delta y = y_0 - y$, were measured when the junctions of the differential thermocouple were spaced at $x = 1.7$ mm (Fig. 7).

The positive value of the temperature gradient $\partial T/\partial x$ decreases with distance from the free surface into the layer and at $\Delta y > 0.75$ mm, $\partial T/\partial x < 0$ during the entire period (Fig. 7). This means that the back-

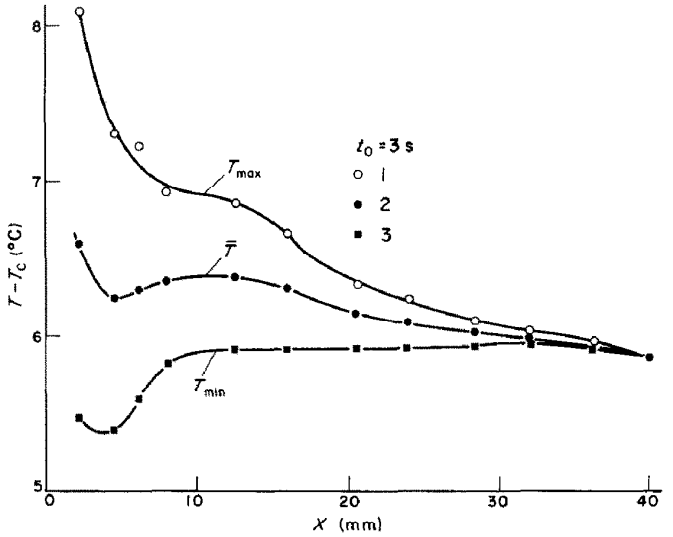

FIG. 5. Maximum (1), mean (2) and minimum (3) periodic temperature fluctuations on a free surface as functions of the distance from the source x. $t_0 = 3$ s.

ward flows ($u < 0$), that originate at $(\partial T/\partial x)_0 > 0$ on the free surface, penetrate to a small depth commensurable with $\Delta y = 0.75$ mm (for $x = 8.7$ mm and $t_0 = 3$ s).

As follows from Fig. 7, the junctions of the differential thermocouple should be located in an exactly horizontal plane ($y = \text{const.}$).

When the junctions of the differential thermocouple are located in one plane $z = \text{const.}$, their mutual effect is possible because of the sweep of perturbations that originate at the thermocouple junction upstream. To eliminate the effect of the junctions on one another, they were located in different planes z, and in this case they were spaced at $\Delta z = 2$ mm.

The longitudinal temperature gradient near the free surface $(\partial T/\partial x)_0$, the velocity gradient $(\partial u/\partial y)_0$ and the friction on the free surface τ_0 (Fig. 8) vary strictly periodically in time at different values of x. When $x < 21$ mm, the quantity $(\partial T/\partial x)_0$ undergoes reversal of sign for the period and, hence, the thermocapillary force vector reverses the direction. Instantaneous values of the friction factor for $x > 21$ mm are always positive. Within the range $4 < x < 13$ mm the mean value of the friction factor $\bar{\tau}_0 < 0$ (Fig. 9),

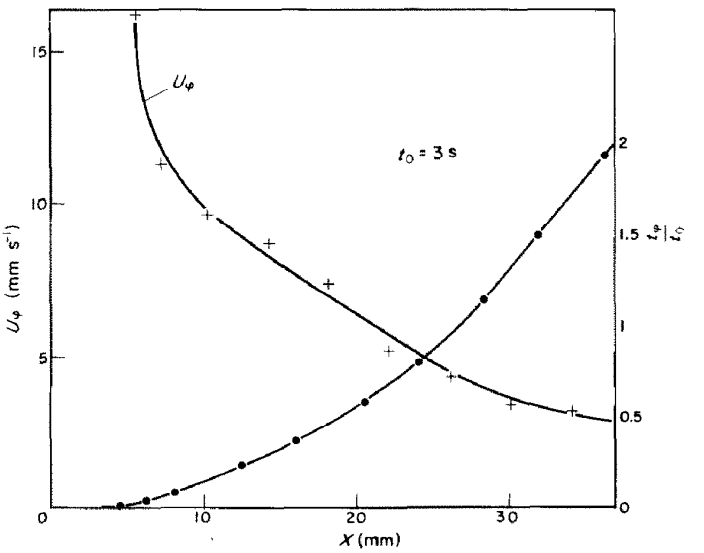

FIG. 6. Dependence of the phase shift and phase velocity of the maximum temperature at $y = 1$ on x. $t_0 = 3$ s.

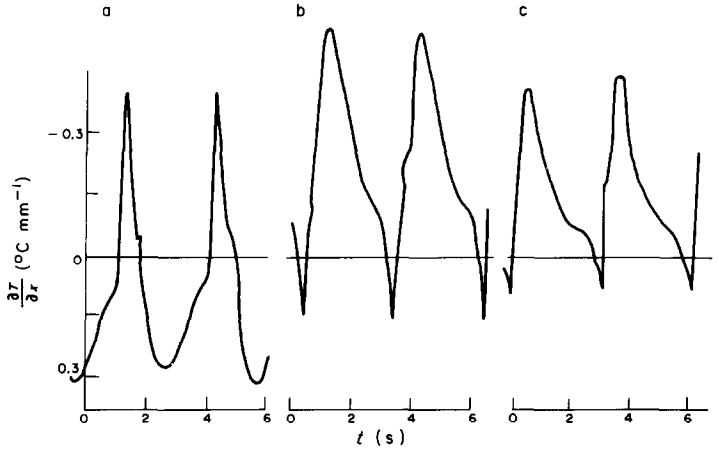

FIG. 7. The horizontal temperature gradient at different distances from the free surface $\Delta y = y_0 - y$ at $x = 8.7$ mm ($t_0 = 3$ s). (a) $\Delta y = 0$; (b) $\Delta y = 0.43$ mm; (c) $\Delta y = 0.75$ mm.

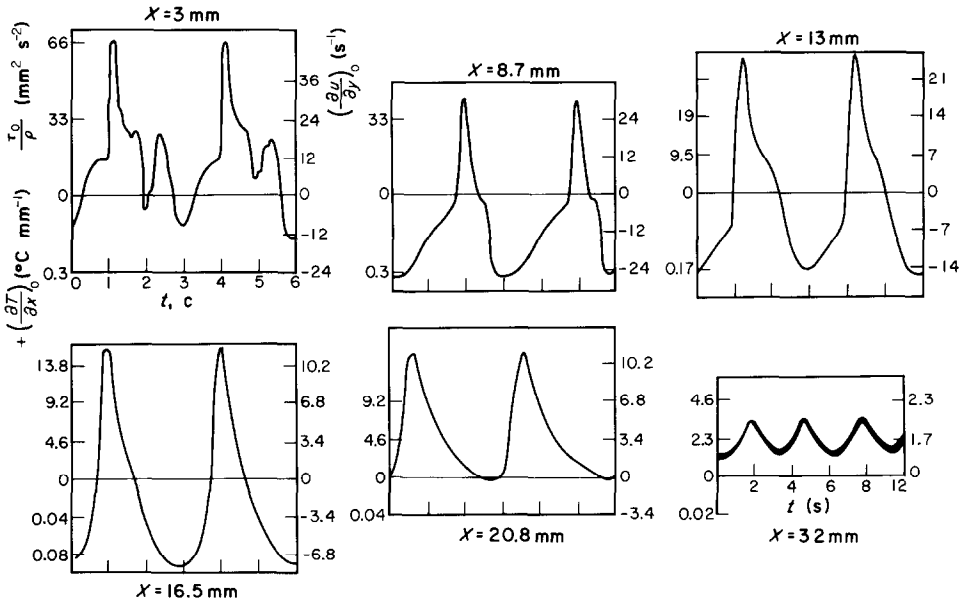

FIG. 8. The longitudinal gradients of temperature $(\partial T/\partial x)_0$ and velocity $(\partial u/\partial y)_0$ and the friction τ_0/ρ on the free surface for different values of x. $t_0 = 3$ s.

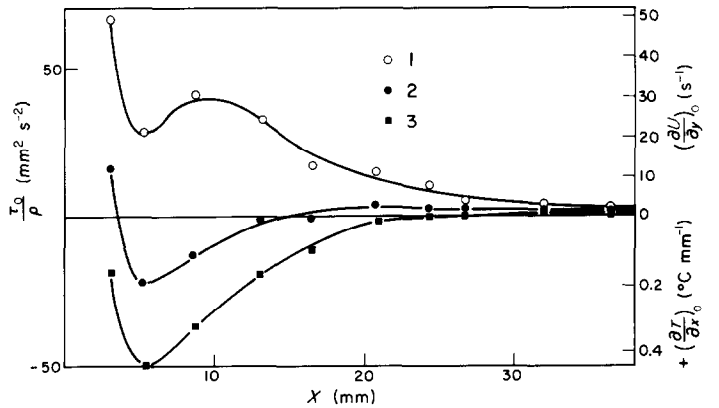

FIG. 9. Maximum (1), mean (2) and minimum (3) values of τ_0/ρ, $(\partial u/\partial y)_0$, $(\partial T/\partial x)_0$ on a free surface. $t_0 = 3$ s.

$(\partial\bar{u}/\partial y)_0 < 0$, and on the free surface the averaged flow is directed toward the heater, this being also confirmed by the measurements of the mean temperature for different values of x (Fig. 5).

Figure 21(b) shows the flow pattern at $t/t_0 = 0.5$ and Q_m. The streamlines could be more clearly seen using an exposure time of about 0.5 s. In the vicinity of the heat source, the flow resembles a vortex which increases periodically up to the greatest dimension $x_a = 3l$ attenuating down to very low velocities. With an increasing frequency of heat flux fluctuations the vortex dimension at $Q = 0$ increases and when $t < 0.1$ s the flow pattern corresponds to the steady-state loading [Fig. 21(a)].

The temperature over the layer thickness for the cross-sections $x = 12.5$ mm and 20.5 mm [Figs. 10(a) and (b)] was measured in the outer region of the greatest vortex: $x = 0.8x_a$ and $1.3x_a$. As is seen from the measurements of the mean maximum and minimum temperatures over the layer thickness [Figs. 11(III) and (IV)], the amplitude of temperature fluctuations varies non-monotonously across the layer: when $1 < y/l < 0.3$ and $-0.2 < y/l < 0.1$, the amplitude of temperature fluctuations increases. The greatest phase shift of T_m at $x = 12.5$ mm amounts to $t_\varphi/t_0 = 0.35$.

In the flow region ($x > 20l$) the experimental velocity and temperature profiles and the temperature gradient correspond to those determined from the solutions of equations (5)–(7) [Figs. 11(I) and (II)].

3. *Periodic flows at* $t_0 = 12$ s

The results of experimental investigations for the conditions: $t_0 = 12$ s, $2l = 9.7$ mm, $\bar{Q} = 27.5$ W m^{-1}, $\Delta T = 2.4$°C, $Ma = -1.1 \times 10^4$, $Ra = 2.37 \times 10^4$, $k = -0.464$, $T_c = 20.1$°C are presented in Figs. 12–18. Knowing the instantaneous temperatures and the phase shift for different values of x (Fig. 12) and also the amplitude and mean values of the temperature (Fig. 13), it is possible to determine the instantaneous values of temperature at any t/t_0 and x on the free surface. Periodic temperature fluctuations near the free surface for $t_0 = 12$ s and $x < 10$ mm have a more complex character than at $t_0 = 3$ s (Figs. 4 and 12).

The mean temperature of the free surface decreases monotonically (Fig. 13). It is possible to distinguish the following regions in the mean temperature behaviour (Fig. 13): the region of a rapid decrease of temperature ($x < 15$ mm) and the region of linear tem-

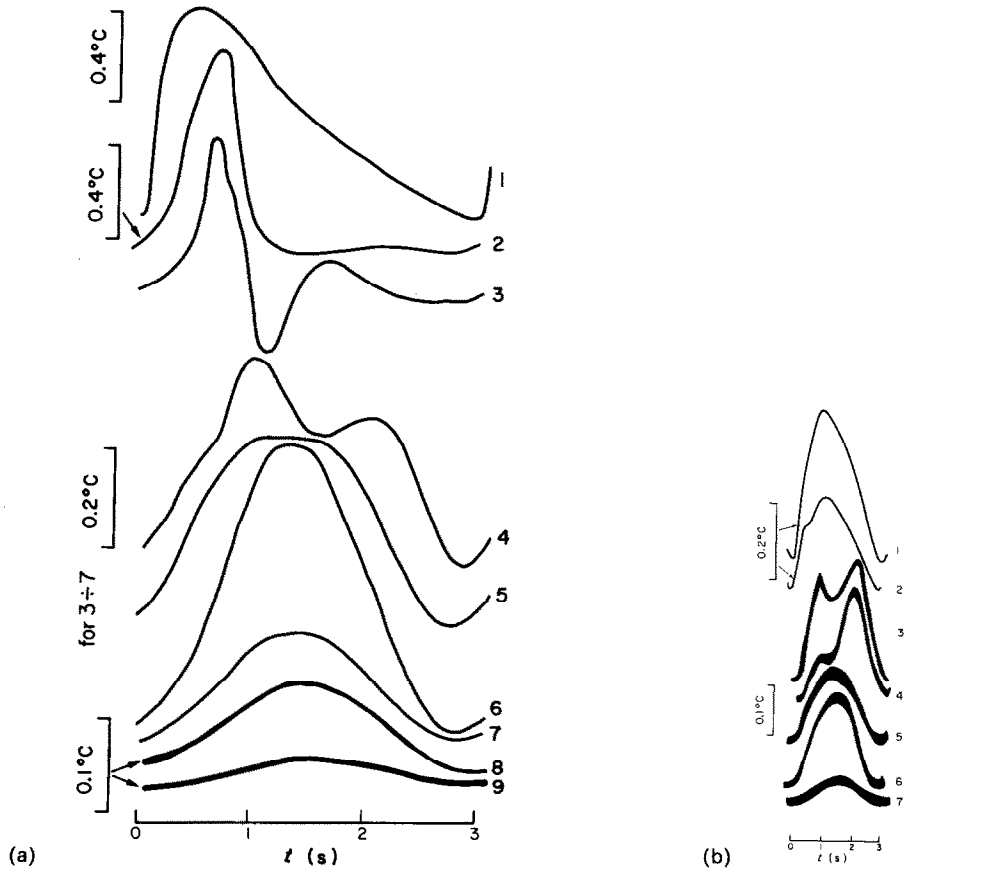

FIG. 10. Time variation of temperature for different values of y. $t_0 = 3$ s. (a) At $x = 12.5$ mm: 1, $y = 1$; 2, $y = 0.79$; 3, $y = 0.56$; 4, $y = 0.39$; 5, $y = 0.27$; 6, $y = 0.07$; 7, $y = -0.17$; 8, $y = -0.33$; 9, $y = -0.51$. (b) At $x = 20.5$ mm: 1, $y = 0.97$; 2, $y = 0.89$; 3, $y = 0.75$; 4, $y = 0.66$; 5, $y = 0.08$; 6, $y = -0.1$; 7, $y = -0.45$.

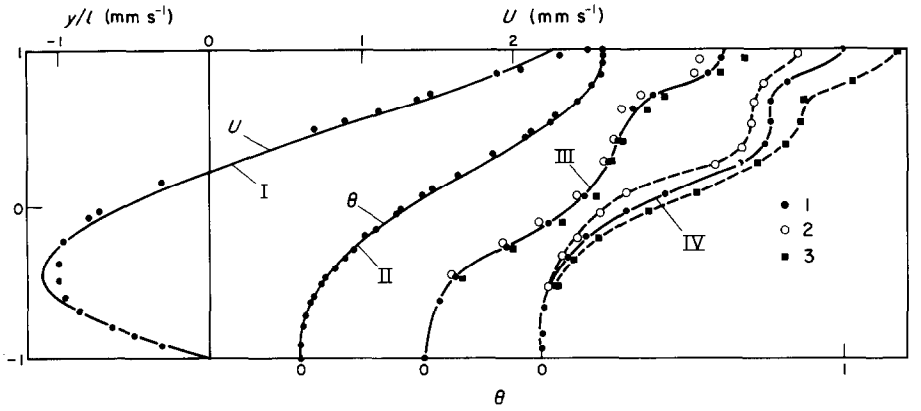

FIG. 11. Temperature and velocity profiles in a layer ($\bar{Q} = 21.04$ W mm^{-1}, $t_0 = 3$ s, $2l = 10.1$ mm). (I) The velocity profile of developed flow. Dots, experimental values at $x = 172$ mm. Line, calculation by equation (6). (II) The temperature profiles from equation (7). Dots, experiment at $x = 172$ mm, $\Delta T = 2°C$, $T_0 = 4.8°C$. (III) The profiles of mean (1), minimum (2) and maximum (3) temperatures at $x = 20.5$ mm, $\Delta T = 2.58°C$, $\bar{T}_0 = 6.3°C$. (IV) The profiles of mean (1), minimum (2) and maximum (3) temperatures at $x = 12.5$ mm, $\Delta\bar{T} = 2.7°C$, $\bar{T}_0 = 6.4°C$.

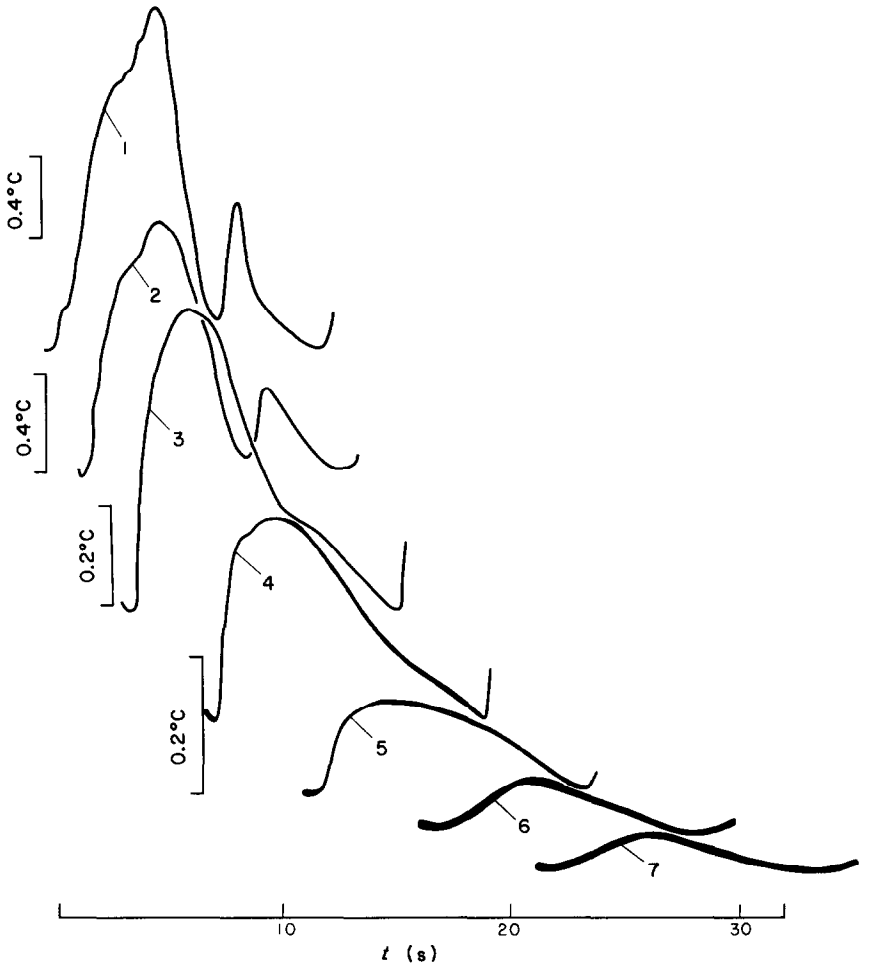

FIG. 12. Free surface temperature variation in time at different distances x from the heater in a horizontal layer: $2l = 9.7$ mm, $\bar{Q} = 27.5$ W m^{-1}, $t_0 = 12$ s, $\Delta T = 2.4°C$, $-Ma = 1.1 \times 10^4$, $Ra = 2.37 \times 10^4$, $k = -0.464$, $T_c = 20.1°C$. (1) $x = 2.25$ mm; (2) 8 mm; (3) 20.25 mm; (4) 47.4 mm; (5) 71.1 mm; (6) 102.7 mm; (7) 142.2 mm.

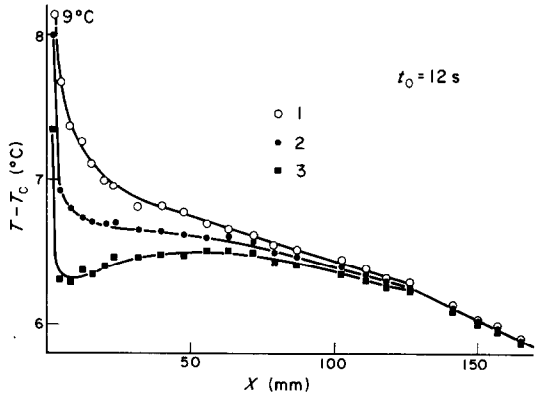

FIG. 13. Maximum (1), mean (2) and minimum (3) temperatures on a free surface at different distances from the heater (x) at $t_0 = 12$ s.

perature variation ($15 < x < 63$ mm, $63 < x < 126$ mm, $x > 126$ mm), in which the temperature gradient $(-\partial T/\partial x)_0$ increases successively up to its value in the developed flow $(-\partial T/\partial x)_0 = 9 \times 10^{-3}$°C mm^{-1} [according to relation (4) the value of the quantity $(-\partial T/\partial x)_0$ is 7.6×10^{-3}°C mm^{-1}].

For the above regions the following trends in the change of the phase velocity of the maximum temperature (Fig. 14) are typical for the above regions: (1) within the region $5 < x < 50$ mm the drop of the phase velocity down to the minimum value $u_\varphi = 4$ mm s^{-1} is observed; (2) within the region $60 < x < 105$ mm the phase velocity increases up to the constant value $u_\varphi = 5$ mm s^{-1}; (3) in the region of $x > 126$ mm the phase velocity increases up to $u_\varphi = 6$ mm s^{-1} and it is higher in magnitude than the free surface velocity $u_0 = 2.5$ mm s^{-1} [Fig. 16(I)].

According to Figs. 13 and 14, an increase of u_φ is connected with an increase in the longitudinal temperature gradient $(-\partial \bar{T}/\partial x)_0$ and, consequently, with an increase of the free surface mean velocity $(\bar{u}_0)$.

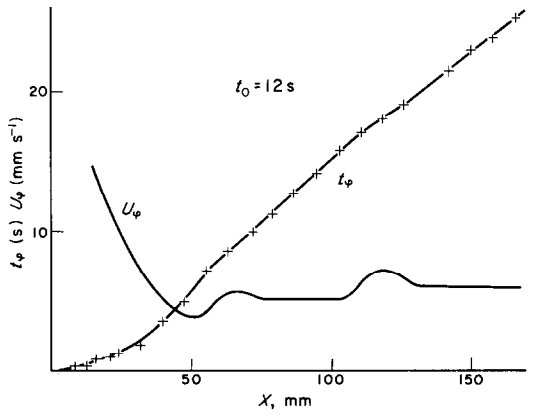

FIG. 14. Dependence of the phase shift and of phase velocity of the maximum temperature at a free surface on x. $t_0 = 12$ s.

It is possible to approximately assume that

$$u_\varphi = u_{\varphi,0} + \bar{u}_0 \tag{10}$$

where $u_{\varphi,0}$ is the phase velocity of the maximum temperature at $(-\partial \bar{T}/\partial x)_0 = 0$. According to equations (5) and (6) the velocity on the free surface can be determined from the relation

$$u_0 = \frac{\beta g l^3}{\nu}\left(-\frac{\partial T}{\partial x}\right)_0\left(\frac{k}{2} - \frac{1}{6}\right) \tag{11}$$

i.e. $u_0 \sim (-\partial T/\partial x)$, other conditions being equal. In the region of $x > 125$ mm, $(-\partial \bar{T}/\partial x)_0 = 0.009$°C mm^{-1} (Fig. 13) and $\bar{u}_0 = 2.5$ mm s^{-1} [Fig. 16(I)]. In the region of $63 < x < 125$ mm, $(-\partial \bar{T}/\partial x)_0 = 0.005$°C mm^{-1} (Fig. 13) and, according to equation (11), $\bar{u}_0 = 1.4$ mm s^{-1}. It follows from relation (10) and Fig. 14 that for the regions with $60 < x < 105$ mm and $128 < x < 170$ mm, $u_{\varphi,0} = 3.5$ mm s^{-1}, i.e. $u_{\varphi,0} =$ const. and the growth of the velocity u_φ is connected with an increase of the free surface velocity. For the case with $t_0 = 3$ s and $\bar{Q} = 21.04$ W m^{-1}, $u_{\varphi,0} = 3.1$ mm s^{-1} (Figs. 5 and 6).

When the maximum temperature phase shifts by a period ($x = 83$ mm), the amplitude of temperature fluctuations on the surface constitutes $0.04\Delta T$ (Figs. 13 and 14); for $x > 130$ mm the amplitude of temperature fluctuations is commensurable with the resolving power of temperature measurements, but it is possible to follow the phase shift of T_m further (Fig. 14).

The longitudinal temperature gradient on the free surface was measured when the junctions of the differential thermocouple were spaced at $\Delta x = 2.25$ mm for $x < 52.5$ mm and at $\Delta x = 3.3$ mm for $x > 52.5$ mm (Fig. 15).

The friction factors τ_0 and $(\partial u/\partial y)_0$ due to thermocapillary forces were calculated by relations (4) from the measured values of $(\partial T/\partial x)_0$. It is seen from Fig. 15 that the quantities $(\partial T/\partial x)_0$, τ_0/ρ, $(\partial u/\partial y)_0$ vary periodically in time for different values of x. The amplitude and mean values of $(\partial T/\partial x)_0$, τ_0/ρ, $(\partial u/\partial y)_0$ are presented in Fig. 16.

When $x < 32$ mm, periodic flows develop on the free surface which are directed to the heater, as can be seen from the negative values of the actual velocity gradient $(\partial u/\partial y)_0$ [Figs. 15, 16 and relations (4)]. In contrast, the mean values of the friction factor $\bar{\tau}_0$ and of $(\partial \bar{u}/\partial y)_0$ are positive at all the xs and the averaged free surface velocity $\bar{u}_0 > 0$ (Fig. 16). This follows also from the mean temperature measurements on the free surface (Fig. 13) and from relations (4) according to which the quantity $(\partial \bar{T}/\partial x)_0$ is negative at all xs and, consequently, $\bar{\tau} > 0$ and $(\partial \bar{u}/\partial y)_0 > 0$. In the region where thermocapillary periodic flows attenuate ($x = 100$ mm, Fig. 16), $(\partial u/\partial y)_0 = 1$ s^{-1}. In the case of a developed plane-parallel flow the velocity gradient due to thermocapillary forces, $(\partial u/\partial y)_0$, is equal to 0.73 s^{-1} (Fig. 18(I)).

Figures 21(c)–(f) present the patterns of flow for

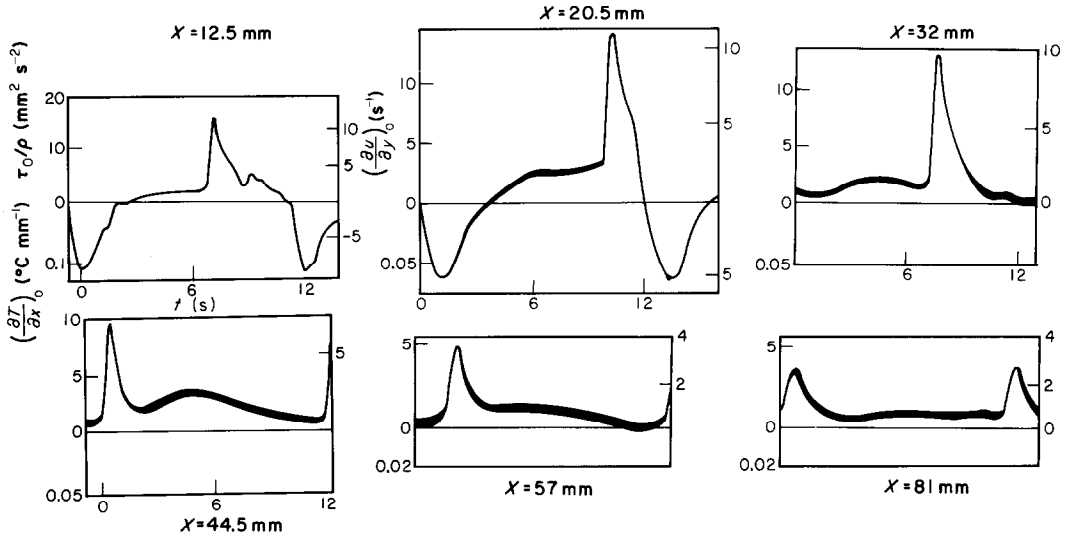

FIG. 15. The longitudinal temperature gradient $(\partial T/\partial x)_0$, velocity gradient $(\partial u/\partial y)_0$ and the friction τ_0/ρ at a free surface as functions of x. $t_0 = 12$ s.

$t/t_0 = 0$, 1/4, 1/2, 3/4, respectively. The time of exposure was about 0.8 s. The flow is of periodic character. When $t \geqslant 0$ ($Q \geqslant 0$) a vortex near the heater [Fig. 23(c)] originates which increases in size at $t/t_0 = 1/4$ [Fig. 21(d)]. At $t/t_0 = 1/2$ ($Q_m = 2\bar{Q}$) a complex multi-vortex structure is observed [Fig. 21(e)]. As the loading decreases ($Q = \bar{Q}$), a one-vortex flow develops near the heater [Fig. 21(f)] which decays because of viscous dissipation, but not completely [Fig. 21(c)].

Temperature fluctuations over the layer thickness were measured for two cross-sections: $x = 18.25$ [Fig. 17(a)] and $x = 31.6$ mm [Fig. 17(c)]. With distance from the free surface ($x = 18.25$ mm), the temperature fluctuations have a complex, but periodic, character: at $y = 0.78$–0.41 high-frequency components appear relative to the base frequency $f = 1/12$ Hz. This seems to be associated with the process of the development and decay of large-scale vortex flow [Figs. 21(c)–(f)]. When $y < -0.76$, a 180° phase shift of T_m is observed. At the cross-section $x = 6.5l$ [Fig. 17(b)] the temperature fluctuations have a strict periodic character and when $y < -0.6$, a 180° phase shift is observed.

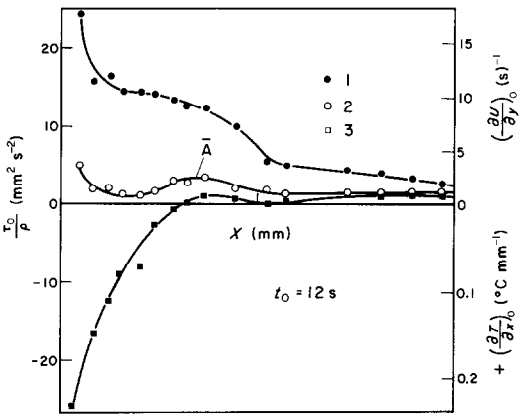

FIG. 16. Maximum (1), mean (2) and minimum values of τ_0/ρ, $(\partial u/\partial y)_0$, $(\partial T/\partial x)_0$ on a free surface. $t_0 = 12$ s.

Mean, maximum and minimum temperatures over the layer thickness at different distances from the heater are presented in Figs. 18(III) and (IV). When $y > 0.9$, the amplitude of temperature fluctuations varies insignificantly and, consequently, the free surface temperature can be measured rather accurately [Figs. 18(III) and (IV)]. At the junction of two flow regions an increase in the amplitude of temperature fluctuations is observed [$y = -0.3$; $x = 18.25$ mm; Fig. 18(IV); Figs. 21(c)–(f)].

Far from the heater, the temperature and velocity profiles have a developed steady-state character and here the solutions (5)–(7) are valid [Figs. 18(I) and (II)].

4. *The limit of propagation of periodic flows* (x_0)

As is shown by investigation, periodic flows mainly decay in a time commensurable with the period of heat flux fluctuation. For example, when $t_0 = 3$ s, $\bar{Q} = 21.04$ W m^{-1} and the maximum temperature phase shifts by one period ($t_\varphi/t_0 = 1$), to which there corresponds $x = 27.5$ mm, the amplitude of temperature fluctuations $\Delta T_m = T_{max} - T_{min}$ is equal to 0.2°C which constitutes 7% of the amplitude ΔT_m at $x = 2.25$ mm (Figs. 5 and 6); for $t_0 = 12$ s, $\bar{Q} = 27.5$ W m^{-1} and the phase shift $t_\varphi/t_0 = 1$ ($x = 83$ mm), $\Delta T_m = 0.1$°C which constitutes only 6% of the amplitude at $x = 2.25$ mm (Figs. 13 and 14). It will be assumed as a first approximation that the path of a periodic perturbation near the free surface x_0 (from

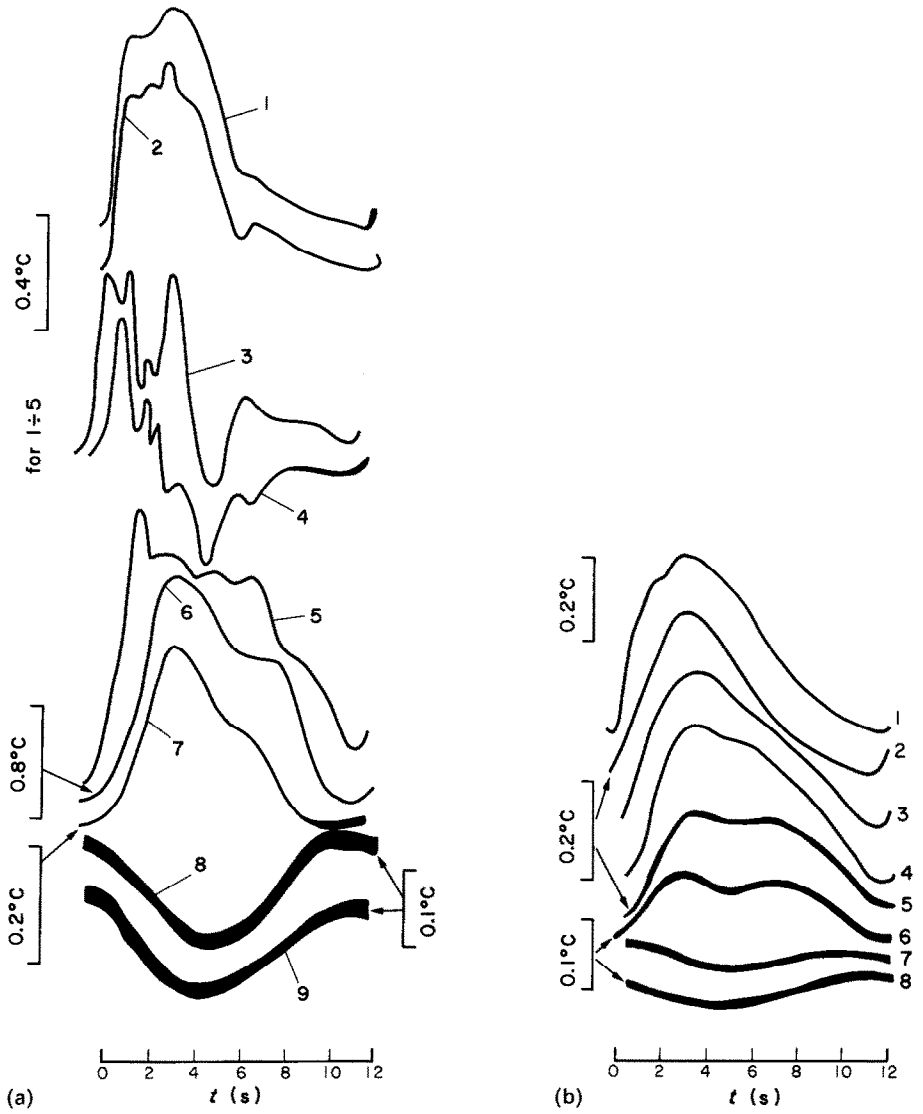

FIG. 17. Periodic variations of temperature ($t_0 = 12$ s) depending on y. (a) At $x = 18.25$ mm: 1, $y = 0.97$; 2, $y = 0.89$; 3, $y = 0.78$; 4, $y = 0.41$; 5, $y = -0.014$; 6, $y = -0.29$; 7, $y = -0.61$; 8, $y = -0.76$; 9, $y = -0.88$. (b) At $x = 31.6$ mm: 1, $y = 1$; 2, $y = 0.42$; 3, $y = 0.22$; 4, $y = -0.16$; 5, $y = -0.35$; 6, $y = -0.49$; 7, $y = -0.68$; 8, $y = -0.81$.

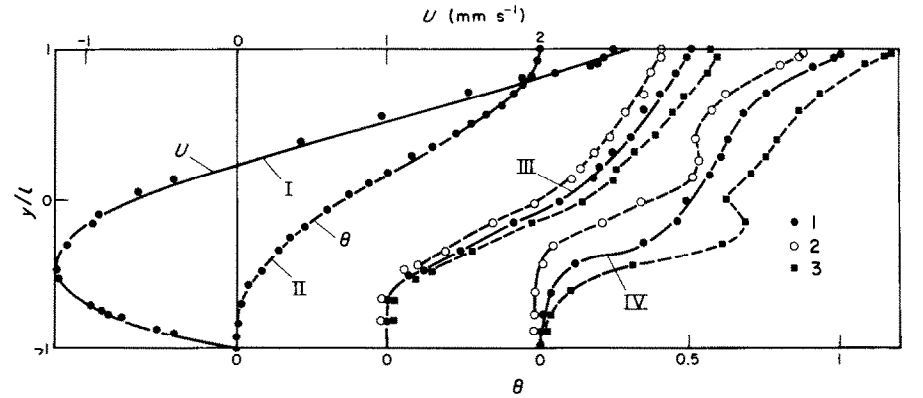

FIG. 18. Temperature and velocity profiles in the layer with $2l = 9.7$ mm, $\bar{Q} = 27.5$ W m^{-1}, $t_0 = 12$ s. (I) The velocity profile of a developed flow. Dots, experimental values at $x = 180$ mm, $\Delta T = 2.4$°C. Line, calculation by equation (6). (II) The temperature profile at $x = 175$ mm, $\Delta\bar{T} = 2.4$°C, $T_0 = 5.8$°C. Line, calculation by equation (7). Dots, experimental values. (III) The profile of mean (1), minimum (2) and maximum (3) temperatures at $x = 31.6$, $\Delta\bar{T} = 2.4$°C, $\bar{T}_0 = 6.65$°C. (IV) The profile of mean (1), minimum (2) and maximum (3) temperatures at $x = 18.25$, $\Delta\bar{T} = 2.6$°C, $\bar{T}_0 = 6.7$°C.

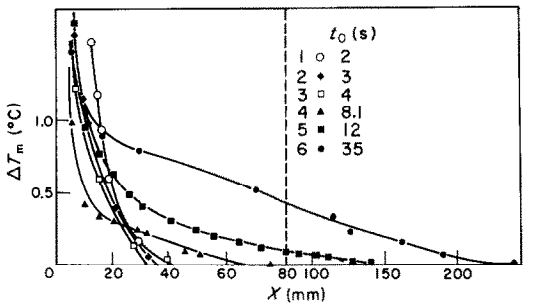

FIG. 19. Dependence of the amplitude of periodic temperature fluctuations on x.

No.	t_0 (s)	$\bar{Q}$ (W m^{-1})	$2l$ (mm)	$Ra \times 10^{-4}$	$-Ma \times 10^{-3}$
1	2	22.5	10.9	2.73	10
2	3	21.04	10.1	2.1	9.2
3	4	14.6	10.4	1.82	7.3
4	8.1	14.6	10.1	1.7	7.1
5	12	27.5	9.7	2.37	11
6	35	22.5	10.9	—	—

the heat source up to complete attenuation) is proportional to the path of a signal in the form of the jump of power $\bar{Q}$ for the time commensurable with the period of heat flux; in this case $x_0 \sim t_0 u_0$. Assume the period of fluctuations to be large enough for the process to be considered quasi-steady at $t = t_0$ and the terms $\partial/\partial t$ to be neglected as compared with the convective terms and the friction force in equations written in the boundary-layer approximation. Then, for adiabatic horizontal surfaces in the absence of the effect of thermogravitational forces ($y = 0$) the velocity scale in the boundary layer near the free surface in the case of thermocapillary convection will be

$$u_0 \sim \left(\frac{b\bar{Q}}{\rho c_p \mu x}\right)^{1/2}. \tag{12}$$

Then the path of attenuation of periodic perturbations is

$$x_0 \sim t_0 \left(\frac{b\bar{Q}}{\rho c_p \mu x_0}\right)^{1/2}. \tag{13}$$

Relation (13) can be restated as

$$t_0^{2/3} \sim x_0 \left(\frac{\rho \mu c_p}{b\bar{Q}}\right)^{1/3} \tag{14}$$

and also as

$$x_0 \left(\frac{\rho \mu c_p}{b\bar{Q} t_0^2}\right)^{1/3} = \text{const}. \tag{15}$$

Figure 19 presents the dependence of the amplitude of periodic perturbations on x for different t_0 and $\bar{Q}$. The length of decay of the periodic perturbation (x_0) was determined from Fig. 19 from the intersection of the averaging relation $\Delta T_m = f(x)$ with the axis x. The results of experimental investigations were presented in the form of relations (14) and (15). It follows from Fig. 20 that

$$x_0(\rho \mu c_p / b\bar{Q} t_0^2)^{1/3} = 2.1;$$
$$x_0(\rho \mu c_p / b\bar{Q})^{1/3} = 2.1 t_0^{2/3}. \tag{16}$$

Thus, according to experimental investigations [Fig. 20, relations (14)–(16)], the propagation of periodic perturbations near a free adiabatic surface is mainly governed by thermocapillary forces. Thermogravitational flows for frequencies above 1/35 Hz are inertial and do not exert a noticeable effect on the attenuation path length (x_0) of periodic thermocapillary flows. In the vicinity of a free, thermally insulated surface, $\partial T/\partial y = 0$, the liquid is in the conditions of neutral stratification and the structure of periodic flow is basically determined by thermocapillary forces. Thermal gravitational forces will influence periodic flows in the layer where $\partial T/\partial y > 0$ and the conditions for stable stratification are present.

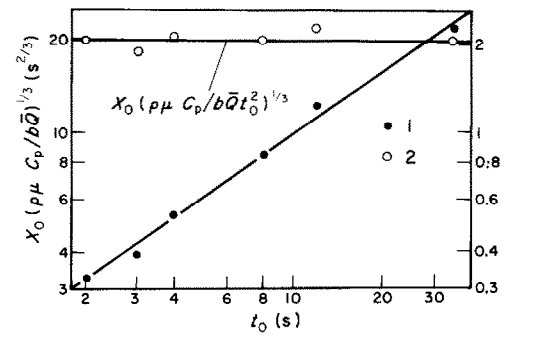

FIG. 20. Dependence of the path of attenuation of periodic perturbations on the period t_0 and amplitude of the power Q. 1 and 2, experimental values.

CONCLUSIONS

In the conditions of periodic flow the interaction of thermocapillary and thermogravitational forces appears to be complex because of different inertias: at large values of t_0 the structure of flows is determined by the interaction of these forces, with the trends in this interaction for $t_0 \to \infty$ corresponding to those of the steady-state flow.

It is shown experimentally that for $t_0 < 35$ s the propagation of periodic flow is mainly determined by thermocapillary forces, whereas the steady-state flow is determined by the interaction of thermocapillary and thermogravitational forces. The structure of thermocapillary periodic flows has been studied.

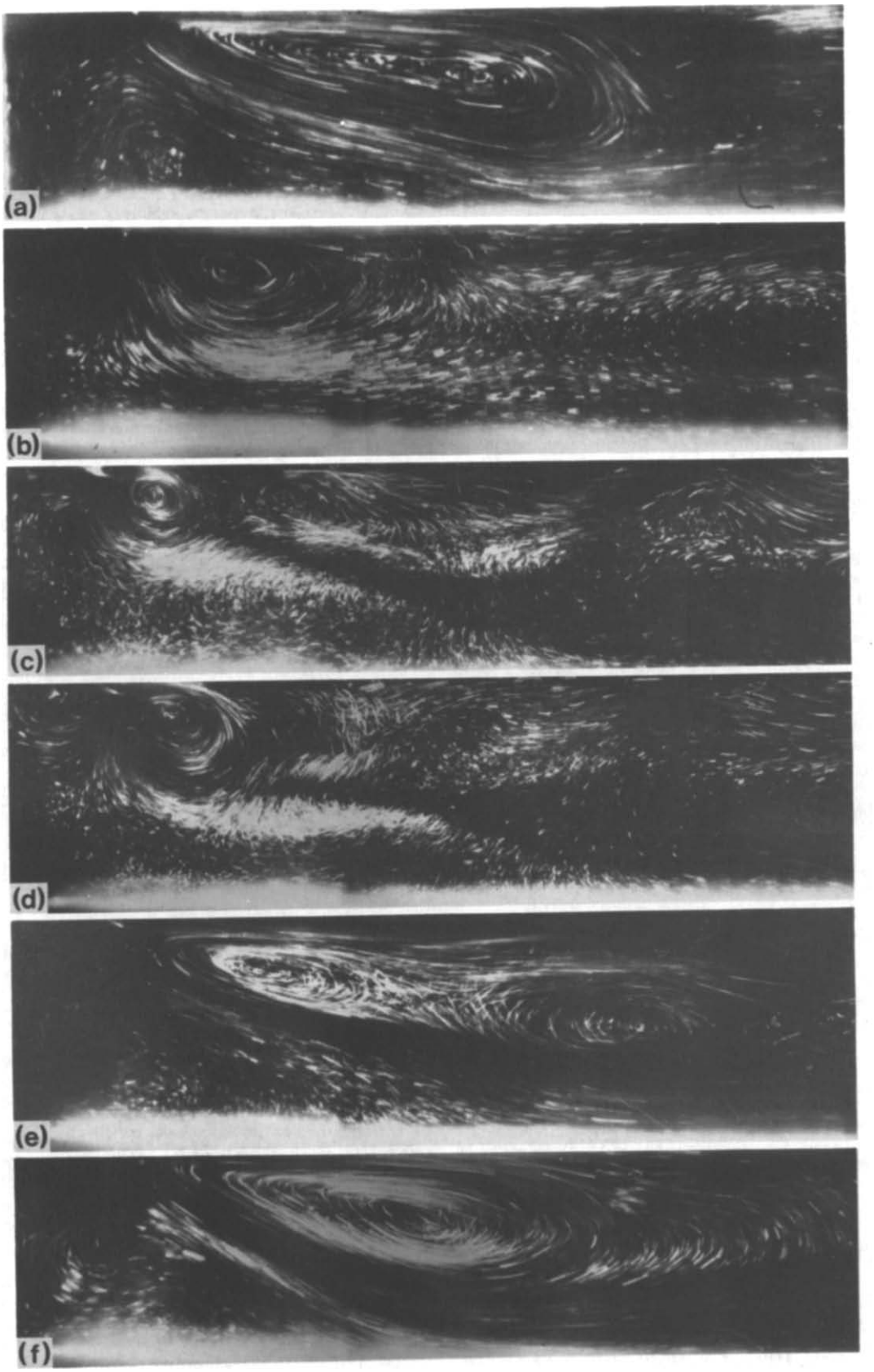

FIG. 21. The fluid flow patterns near the heater. (a) Steady-state power $\bar{Q} = 21$ W m^{-1}, $2l = 10.1$ mm. (b) Periodic power at time $t = t_o/2$, $t_o = 3$ s, $\bar{Q} = 21.04$ W m^{-1}, $2l = 10.1$ mm, $Ra = 2.1 \times 10^4$, $Ma = -9.2 \times 10^3$. Periodic power $\bar{Q} = 27.5$ W m^{-1}, $t_o = 12$ s, $Ra = 2.37 \times 10^4$, $Ma = -1.1 \times 10^4$. (c) $t = 0$. (d) $t_o = t_o/4$. (e) $t = t_o/2$. (f) $t = 3t_o/4$.

Acknowledgements—The author is grateful to V. F. Zaporozhko for building the experimental setup which has allowed this investigation to be carried out, and to V. K. Kovriguina for the help rendered in paper preparation.

REFERENCES

1. R. V. Birikh, Concerning the thermocapillary convection in a horizontal layer of liquid, *Prikl. Mat. Tekh. Fiz.* No. 3, 67–72 (1966).
2. A. G. Kirdyashkin, Thermogravitational and thermocapillary flows in a horizontal liquid under the conditions of a horizontal temperature gradient, *Int. J. Heat Mass Transfer* **27**, 1205–1218 (1984).
3. V. I. Polezhayev, Hydrodynamics, heat and mass transfer during the growth of crystals. Advances in science and technology. In *Mechanics of Liquid and Gas*, Vol. 18, pp. 198–296. Moscow (1984).
4. Yu. I. Barkov, The effect of side wall temperature modulation on the structure of convective motion in a horizontal cavity. In *Modern Problems of Thermal Gravitational Convection*, pp. 26–31. Izd. ITMO AN BSSR, Minsk (1974).
5. Yu. I. Barkov, B. M. Berkovsky and V. E. Fertman, Experimental investigation of thermoconvective waves in a horizontal layer of gas, *J. Engng Phys.* **27**, 618–623 (1974).
6. B. M. Berkovsky and A. K. Sinitsyn, Thermoconvective waves in a horizontal cavity, *Izv. Akad. Nauk SSSR, Mekh. Zhidk. Gaza* No. 2, 180–182 (1975).
7. E. F. Nogotov and A. K. Sinitsyn, Thermoconvective waves in a horizontal bounded layer of an incompressible fluid, *J. Engng Phys.* **31**(1), 79–85 (1976).
8. G. Z. Gershuni, E. M. Zhukhovitsky and V. M. Myznikov, The stability of a plane-parallel convective flow of fluid in a horizontal layer with respect to spatial disturbances, *Prikl. Mat. Tekh. Fiz.* No. 5, 145–147 (1974).
9. V. M. Myznikov, About the stability of steady advective motion in a horizontal layer with a free boundary with respect to spatial disturbances. In *Convective Flows*, pp. 76–82. Perm (1981).
10. V. M. Myznikov, Finite-amplitude spatial disturbances of the advective motion in a horizontal layer with a free boundary. In *Convective Flows*, pp. 83–88. Perm (1981).
11. M. Smith and S. H. Davis, Instabilities of dynamic thermocapillary liquid layers, *J. Fluid Mech.* **132**, 119–144 (1983).
12. F. Preisser, D. Schwabe and A. Scharman, Steady and oscillatory thermocapillary convection in liquid columns with free cylindrical surface, *J. Fluid Mech.* **126**, 545–567 (1983).
13. M. Strani, R. Piva and G. Graziani, Thermocapillary convection in a rectangular cavity: asymptotic theory and numerical simulation, *J. Fluid Mech.* **130**, 347–376 (1983).
14. A. G. Kirdyashkin, V. I. Polezhaev and A. I. Fedyushkin, Thermal convection in a horizontal layer with lateral heat supply, *Prikl. Mat. Tekh. Fiz.* No. 6, 122–128 (1983).

ECOULEMENTS PERIODIQUES THERMOCAPILLAIRES

Résumé—On décrit des études expérimentales de la structure des écoulements thermocapillaires périodiques formés à partir de variations périodiques du flux thermique d'une source linéaire située sur une surface libre. Les écoulements périodiques se développent dans une couche plane horizontale avec des surfaces horizontales adiabatiques. Les champs de température sont mesurés à différents instants et amplitudes du changement de flux thermique. Les gradients instantanés et moyens de température sont mesurés le long d'une surface libre et aussi le frottement sur la surface. Les limites de la propagation des perturbations périodiques dépendent de l'amplitude et de la période du changement. On montre que pour $t_0 > 35$ s les forces thermogravitationnelles n'exercent pas un effet sensible sur la propagation d'un écoulement périodique le long de la surface libre.

PERIODISCHE GRENZFLÄCHENSTRÖMUNGEN

Zusammenfassung—In diesem Bericht werden experimentelle Untersuchungen über periodische Grenzflächenströmungen vorgestellt, die durch periodische Variation der Wärmestromdichte einer linienförmigen Quelle an einer freien Oberfläche erzeugt werden. Die periodischen Strömungen entstehen in einer ebenen horizontalen Schicht mit adiabaten horizontalen Begrenzungsflächen, deren Verhalten hinsichtlich Konvektionsströmungen in größerer Entfernung von der Wärmequelle bekannt ist. Es werden die Temperaturfelder bei unterschiedlicher Amplitude und Schwingungsdauer der periodisch wechselnden Wärmestromdichte ermittelt. Momentane und gemittelte Temperaturgradienten entlang einer freien Oberfläche, und damit auch die Reibung, werden gemessen. Die Grenzen der Ausbreitung der periodischen Strömungen werden anhand der Amplituden- und Periodenänderungen ermittelt. Es zeigt sich, daß für Periodendauern von $t_0 < 35$ s Auftriebskräfte keinen entscheidenden Einfluß auf die Ausbreitung einer periodischen Strömung entlang der freien Oberfläche haben.

ТЕРМОКАПИЛЛЯРНЫЕ ПЕРИОДИЧЕСКИЕ ТЕЧЕНИЯ

Аннотация—Представлены экспериментальные исследования структуры периодических термокапиллярных течений, возникающих вследствие периодических изменений тепловой нагрузки на линейном источнике, расположенном у свободной поверхности. Развитие периодических течений происходит в плоском горизонтальном слое с адиабатическими горизонтальными поверхностями, для которого изучены закономерности конвективного течения вдали от источников тепла. Измерены поля температуры при различных периодах и амплитудах изменения тепловой нагрузки. Измерены мгновенные и средние градиенты температуры вдоль свободной поверхности и, следовательно, трение на поверхности. Найдены границы распространения периодических возмущений в зависимости от амплитуды и периода изменения нагрузки. Показано, что при $t_0 < 35$ с термогравитационные силы не оказывают заметного влияния на распространение периодического течения вдоль свободной поверхности.